10

A Climbing Robot for Cleaning Glass Surface with Motion Planning and Visual Sensing

Dong Sun, Jian Zhu and Shiu Kit Tso
Department of Manufacturing Engineering and Engineering Management
*City University of Hong Kong*
Hong Kong

1. Introduction

There exists increasing demand for the development of various service robots to relieve human beings from hazardous jobs, such as cleaning glass-surface of skyscrapers, fire rescue, and inspection of high pipes and walls (Balaguer et al., 2000; La Rosa et al., 2002; Zhu et al., 2002). Fig. 1 shows our recently developed climbing robotic system aimed to clean glasses of high-rise buildings, using suction cups for adhering to the glass and a translation mechanism for moving. This robot can reach a maximum speed of 3 m/min and has the ability to cross cracks and obstacles less than 35mm in height and 80mm in width. Utilizing a flexible waist, the robot can easily adjust its orientation.

Motion planning of the service robot plays an important role to enable the robot to arrive in the target position and avoid or cross obstacles in the trajectory path. There are considerable approaches in the literature to address the motion planning problem of car-like or walking robots, such as Lamiraux and Laumond (2001), Boissonnat etc. (2000), Hasegawa etc. (2000), Chen et al. (1999), Hert and Lumelsky (1999), Egerstedt and Hu (2002), Mosemann and Wahl (2001), to name a few. All these algorithms are not suitable to our cleaning robot applications. This is because 1) the movement mechanism of the climbing robot uses translational suction cups, which is different from the other robots; and 2) the climbing robot works in a special environment, i.e., the glass wall, which is divided into many rectangle sections by horizontal and vertical window frames, and the robot must be able to cross the window frames to clean all sections. Because of these characteristics, there exists a demand for a unique motion planning scheme for the climbing robot application.

Another key issue to the success of the climbing robot application lies in an effective sensing capability. To do the cleaning work on the glass surface, the cleaning robot must know when to begin or stop the cleaning job, how to control the orientation (or moving direction), and how to cross the window frame. Therefore, it is necessary to measure the robot orientation, the distance between the robot and the window frame, and the distance between the robot and the dirty spot to be cleaned. Some recent works on the sensing system of cleaning robots have been reported in the literature (Malis et al., 1999; Ma et al., 1999). Simoncelli et al. (2000) utilized the ultrasonic sonar for automatic localization. Kurazume and Hirose (2000) proposed the so-called "cooperative positioning system" to

repeat a searching process until the target position was reached. However, in a climbing robot on the glass surface, many traditional methodologies with laser and ultrasonic sensors etc. cannot be applicable to measure the distance between the robot and the window frame. This is because that the height of the window frame is usually low and the light beam sent by the sensor is difficult to reach the frame unless the beam is exactly parallel to the glass surface. Due to inevitable installation errors, the sensors are usually hard to ensure that the light beam is parallel to the glass surface exactly. Cameras are often used for the robot's localization, visual servoing, and vision guidance. Malis et al. (2000) used two cameras for 2-D and 2-1/2-D visual servoing and proposed a multi-camera visual servoing method. However, the use of a number of cameras may not be suitable to the climbing robot because 1), it is difficult to establish a big zone of intersection of points of view when using several cameras, and 2), using a number of cameras increases the load weight and thus affects the safety of the climbing robot. Based on eigenspace analysis, a single camera was used to locate the robot by orienting the camera in multiple directions from one position (Maeda et al., 1997). The drawback of this eigenspace method is that the measuring performance may vary as environment changes. In addition, the depth information is lost and the distance between the camera and the target object cannot be measured by traditional single camera.
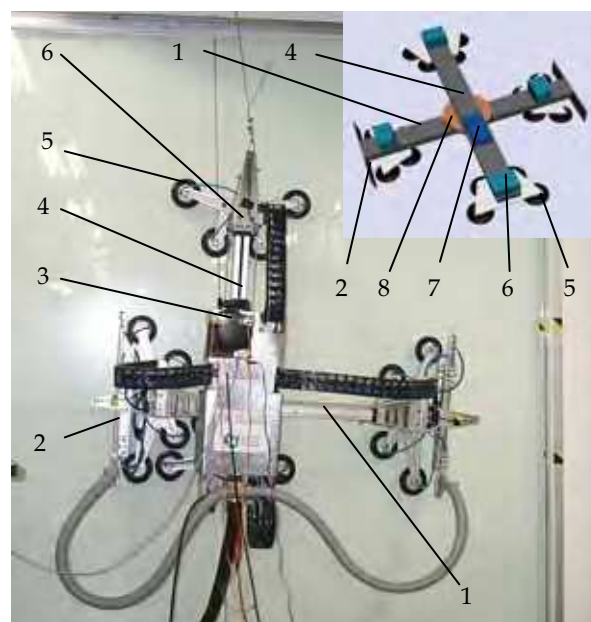
1. Horizontal (X-) Cylinder   2. Brush
3. Visual Sensor   4. Vertical (Y-) Cylinder
5. Suction Cup   6. Z-Cylinder
7. Slave CPU   8. Rotation Cylinder

Fig. 1. Main structure of the climbing robot

This chapter presents our approaches to solving the above two challenging problems, motion planning and visual sensing, for a climbing glass-cleaning robot. Some works have been reported in Zhu etc. (2003) and Sun etc. (2004). The reminder of the chapter is organized as follows. In section 2, structure of the climbing robot is introduced. In section 3, mtion planning of the robot on a multi-frame galss wall is presented. In section 4, a visual sensing system that is composed of an omnidirectional CCD camera and two laser diodes, is shown to enable the robot to measure its orientation and the distance between the robot and the window frame. Experiments are performed in section 5 to demonstrate the effectiveness of the proposed approach. Finally, conclusions of this work are given in section 6.

2. Structure of the Cleaning Robot

The cleaning robotic system consists of a mobile climbing robot, a supporting vehicle, a compressor, and a computer. The climbing robot sticks on the glass surface to perform the cleaning job. The supporting vehicle supplies electrical power and cleaning liquid. The compressor acts as the air source. Through communication between the computer and the robot, the human operator can examine and control the operation of the robot.
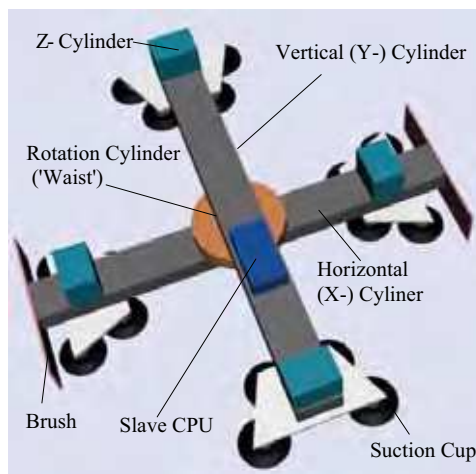

Fig. 2. Main structure of the climbing robot

The developed climbing robot has a length of 1220 mm, a width of 1340 mm, a height of 370 mm, and a weight of 30 Kg. The body of the robot is mainly composed of two rodless cylinders perpendicular to each other, as shown in Fig. 1. The stroke of the horizontal (X-) cylinder is 400mm, and that of the vertical (Y-) cylinder is 500mm. Actuating these two cylinders alternately, the robot moves in the X or Y direction. As shown in Fig. 2, four short Z- cylinders are installed at the two ends of each rodless cylinder. By stretching out or drawing back the piston beams of these four cylinders, the robot can move in the Z direction. At the intersection of two rodless cylinders, a rotational cylinder named the robot's waist is installed, by which the robot can rotate around the Z-pivot. Two specially designed brushes, each composed of a squeegee and a sucking system, are fixed at the two

ends of the horizontal cylinder. The squeegee cleans dirty spots on the glass surface using cleaning liquid provided by the supporting vehicle. The sucking system collects and returns the sewage to the supporting vehicle for recycling.

The robot employs suction pads for adhesion. Four suction pads, each with a diameter of 100mm, are installed on each foot of the robot. The total sixteen pads provide a suction force enough to withstand 15 Kg payload. The robot uses a translational mechanism for the movement. With the operating mode of sticking-moving-sticking, the robot can complete a series of motions including moving, rotation, and crossing obstacles. The rotation of the robot is controlled by adjusting rotation angles of the rotational cylinder. The robot can rotate 1.6 degrees per step around Z-pivot until reaching the desired posture.

The control system of the robot is based on a master and a slave computer. The master computer is located on the ground and manipulated by the human operator directly. The slave computer is embedded in the body of the robot. Using the feedback signal of sensors installed on the robot, the slave computer controls the movement and the posture of the robot to achieve automatic navigation on the glass surface. The master computer obtains the information and identifies the status of the robot by the visual sensing system together with the communication between the master and the slave computers with a RS422 link. In case of emergency, the human operator can directly control the robot according to the actual situation.

The movement of the robot is achieved by alternately sucking and releasing the suction cups installed on the horizontal and vertical rodless cylinders. The slave computer sends ON or OFF signals to connect or disconnect the vacuum generator with air source, resulting in sucking or releasing the corresponding suction cups. Vacuum meters measure the relative vacuum of the suction cups and check the safety of the robot. If the vacuum degree of the suction cups is less than -40 kPa, an alarm signal is sent to the master computer.

Fig. 3 illustrates the developed cleaning robot climbing on the commercial building of City Plaza in Hong Kong.

Fig. 3. The climbing robot on site trial outside a commercial building (provided by BBC)

3. Motion Planning

For simplicity, the robot moves horizontally and vertically to clean the whole glass surface in the motion planning. As an example, Fig. 4 illustrates a trajectory path of the robot within a rectangular glass section. The starting point is located in the up-right side of the glass section. The robot moves toward the left side horizontally while cleaning the glass surface. When arriving at the boundary of the glass section, the robot moves down a distance l and then moves back to the right side horizontally. Note that the distance l is equal to the length l_b of the brush cleaning path, and l_b is determined by considering the size of the brush and the dimension of the glass section. Repeating the above procedures, the whole glass section can be cleaned. The ending position is located in the down side of the glass section. During cleaning the sewage may drop down and makes the downside glass surface dirty. Therefore, the cleaning work should be performed from the upside to the downside.
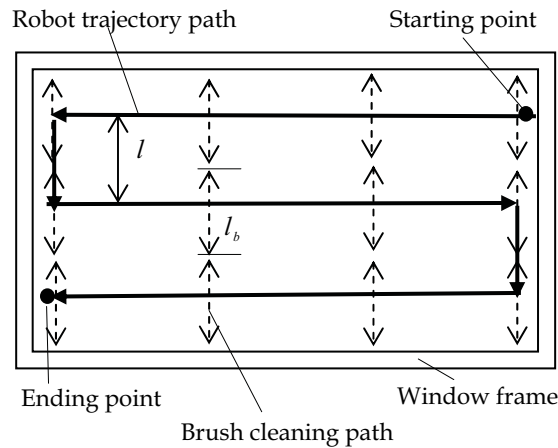

Fig. 4. Robot motion path on the glass

3.1 Orientation Adjustment of the Robot

When the climbing robot moves along the desired trajectory, the robot orientation is affected by various disturbances, especially by the gravitational force of the robot itself. To ensure a successful trajectory following, the robot must be able to adjust its orientation automatically. The orientation of the robot is measured by the visual sensor installed on the robot, relative to the window frame. Two laser diodes send two laser lights to the window frame so that an image of the frame can be acquired. The orientation of the robot relative to the window frame can be calculated by analyzing and comparing the image coordinates of two laser points. The technical details of this measurement are given in the next section.

Based on the orientation measured by the visual sensor, the controller actuates the rotational cylinder to adjust the orientation of the robot. The orientation is adjusted by the sticking-releasing-sticking mode, as shown in Fig. 5. Firstly, the suction cups installed on the vertical cylinder are released (see Fig. 5 (1)). Secondly, the rotational cylinder is actuated to rotate the vertical cylinder (see Fig. 5 (2)). Then, the suction cups on the vertical cylinder are sucked, and meanwhile, the suction cups on the horizontal cylinder are released (see Fig. 5

(3)). Finally, the rotational cylinder is actuated again to rotate the horizontal cylinder (see Fig. 5 (4)).
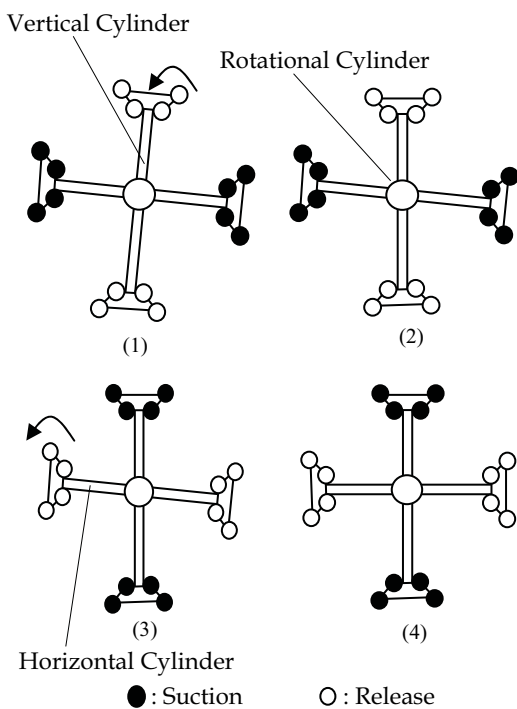
Vertical Cylinder

Rotational Cylinder

(1)   (2)

(3)   (4)

Horizontal Cylinder

● : Suction   ○ : Release

Fig. 5. Rotation of the robot

3.2 Crossing the Window Frame

Horizontal Window Frame   Vertical Window Frame

Section 3   Section 2   Section 1

Section 4   Section 5   Section 6

d
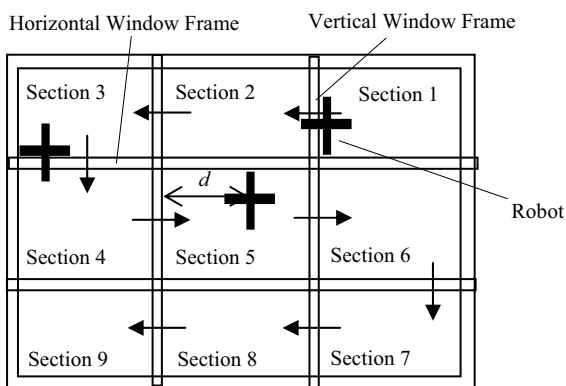
Robot

Section 9   Section 8   Section 7

Fig. 6. Path planning of the climbing robot in a multi-frame glass wall

The window frames separate the whole glass wall into several sections, as shown in Fig. 6. After cleaning one section, the robot must be able to cross the vertical or horizontal window frame to enter another section. The two major steps for the robot to cross the window frame are:

1) Measuring the distance between the robot and the window frame

The distance between the robot and the window frame, denoted by d as seen in Fig. 6, is an important factor to evaluate the position of the robot in each section. When this distance is close to zero, the robot prepares to cross the window frame. The visual sensor is employed to measure the distance between the robot and the window frame. According to the theory of triangulation, one laser diode is needed to measure the distance. The distance is measured by analysis and calculation of the pixel coordinate of the laser point, based on the position and posture of the CCD camera relative to the laser diode, which will be shown in the next section.
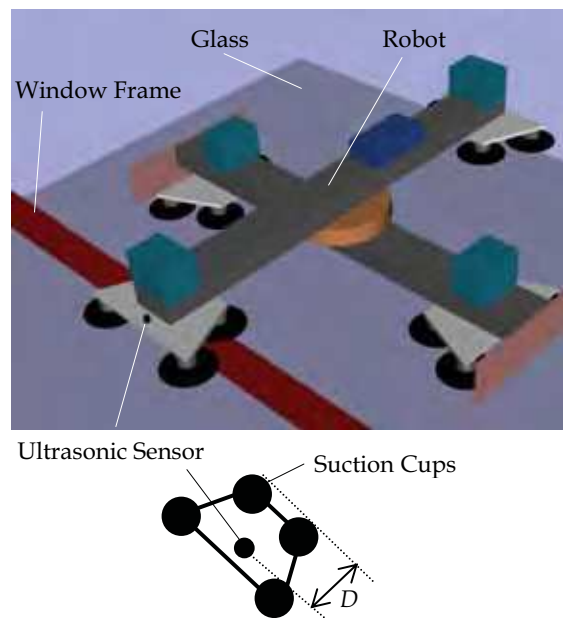

Fig. 7. Ultrasonic sensors installed on the robot

2) Crossing the window frame

After measuring the distance between the robot and the window frame, the robot plans its motion to cross the frame. Four ultrasonic sensors are installed to help the robot to detect whether the suction cups have crossed the window frame, as shown in Fig. 7, where D (=300mm) denotes the distance between the ultrasonic sensor and the boundary of suction cups. When the ultrasonic sensor is crossing the window frame, the ultrasonic sensor measures the height of its position relative to the surface of the window frame. After the ultrasonic sensor crosses the window frame, the height measured by the ultrasonic sensor is the one relative to the glass surface. Since the height measurements in the two cases are

different, the robot knows whether the ultrasonic sensor has crossed the window frame. When the ultrasonic sensor lies in the window frame, the robot also knows when the suction cups will follow the ultrasonic sensor to cross the window frame after moving a distance D.

4. Visual Sensing

The visual sensing hardware system consists of an oriented CCD camera with the model number Sony EVI-D30 (J), two laser diodes, and a capture card. Two laser diodes, fixed on the camera as "eyes" of the sensing system, send two laser lights to find the window frame and generate two laser marks. The distances between the reference points and the window frame, and the orientation of the robot relative to the window frame, can be determined by analyzing image pixel coordinates u and v of two laser points in the image plane.
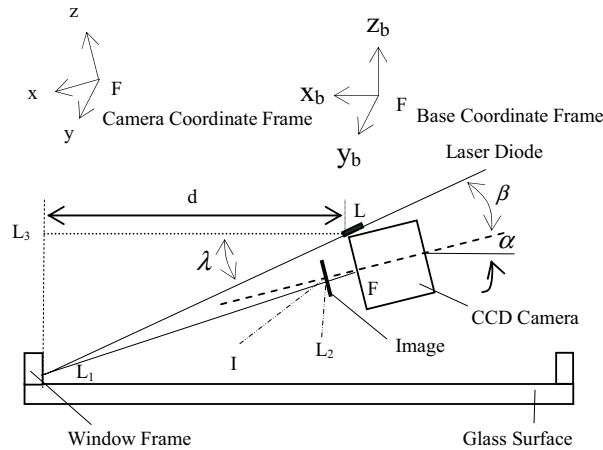

Fig. 8. Measurement of the robot position

4.1 Position Measurement

The theory of triangulation will be utilized in the measurement. Fig. 8 (left view) illustrates how the robot position is measured by the visual sensing system. The launching point of the laser diode is represented by L. Point L_1 is the laser mark on the window frame. Point L_2 is the corresponding point of L_1 in the image plane, where I denotes the center of the image. Treating the focal point of the camera as the origin, denoted by F, a base coordinate frame represented by F-$x_b y_b z_b$ is established, where x_b coordinate axis is parallel to the glass surface and perpendicular to the window frame, y_b coordinate axis is parallel to both the window frame and the glass surface, and z_b coordinate axis is perpendicular to the glass surface(x_b-y_b plane), as shown in Fig. 8. Using F as the same origin, another coordinate frame named camera coordinate frame, represented by F-xyz, is also established, where x axis is parallel to line I-F that is the main light pivot of the camera, y axis is the same as y_b axis of the base coordinate frame, and z axis is perpendicular to the x-y plane. Denote $[x_0, y_0, z_0]^T$, $[x_1, y_1, z_1]^T$ and $[x_2, y_2, z_2]^T$ as coordinates of the points L, L_1 and L_2, respectively. Denote u

and v as coordinates in pixel in the image plane, and u_0 and v_0 as the pixel coordinates of the central point I.

Since the focal point F is located in the line L_1-L_2, the line L_1-L_2 can be represented by

$$\frac{x}{x_2} = \frac{y}{y_2} = \frac{z}{z_2} \tag{1}$$

Define β as the tilt angle of the laser diode relative to the camera (around y axis, anti-clockwise), γ as the pan angle (around z axis, anti-clockwise). Then, the line L-L_1 can be represented by

$$\frac{x - x_0}{1} = \frac{y - y_0}{tg\gamma} = \frac{z - z_0}{-tg\beta} \tag{2}$$

From (1) and (2), we can derive coordinates of point L_1 in pixel coordinate u, i.e.,

$$[x_1, y_1, z_1]^T = K_u + [x_0, y_0, z_0]^T \tag{3}$$

where $K_u = \begin{bmatrix} \dfrac{-x_0 d_x(u-u_0) - y_0 f}{d_x(u-u_0) + f\,tg\gamma} \\[2mm] \dfrac{-x_0 d_x(u-u_0)tg\gamma - y_0 f\,tg\gamma}{d_x(u-u_0) + ftg\gamma} \\[2mm] \dfrac{x_0 d_x(u-u_0)tg\beta + y_0 f\,tg\beta}{d_x(u-u_0) + ftg\gamma} \end{bmatrix}$, in which d_x and d_y are distances between two

adjacent pixels in two directions of the image plane, and f denotes the focal distance.

The distance between L and L_1, represented by $|LL_1|$, is

$$|LL_1| = \sqrt{(x_1 - x_0)^2 + (y_1 - y_0)^2 + (z_1 - z_0)^2} \tag{4}$$

Define α as the tilt angle of the camera in the base coordinate frame. The angle between the line L-L_1 and the line L-L_3 (parallel to x_b axis) is

$$\lambda = \arccos(\frac{\cos\alpha - \sin\alpha\,tg\beta}{\sqrt{1 + tg^2\beta + tg^2\gamma}}) \tag{5}$$

Then, the distance between point L and the window frame is

$$d = |LL_1|\cos\lambda \tag{6}$$

Substituting (3), (4) and (5) into (6) yields d in pixel coordinate u, i.e.,

$$d = \frac{a_1 u + a_2}{u + a_3} \cos(\alpha + \beta) \tag{7}$$

where $a_1 = \frac{-x_0}{\cos\beta}$, $a_2 = \frac{x_0 u_0 d_x - y_0 f}{\cos\beta\, d_x}$, and $a_3 = \frac{-u_0 d_x + f t g \gamma}{d_x}$.

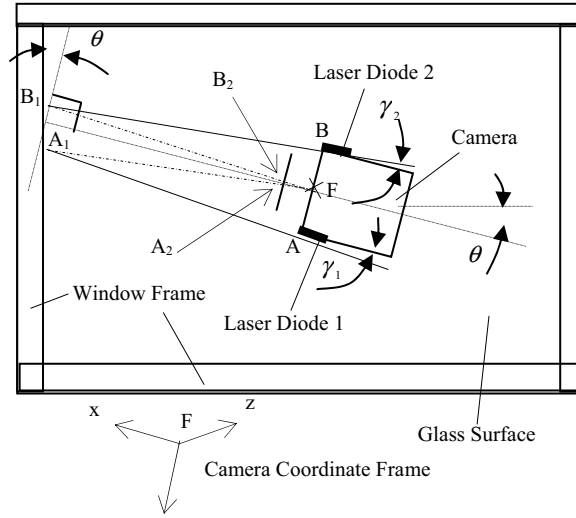In a similar manner, the distance d can be derived as the function of the pixel coordinate v.

Fig. 9. Measurement of the robot orientation

4.2 Orientation Measurement

Fig. 9 (front view) illustrates a measurement of the robot orientation using the visual sensing system, where two laser diodes are needed. Points A and B are launching points of laser diodes 1 and 2, respectively. Points A_1 and B_1 are the corresponding laser marks in the window frame. γ_1 and γ_2 are the pan angles of laser diodes 1 and 2 relative to the camera. Denote the positions of the left point A and the right point B in the camera coordinate frame by $[x_L, y_L, z_L]^T$ and $[x_R, y_R, z_R]^T$, respectively. In the x-y plane, the line A-A_1 is represented by

$$\frac{y - y_L}{\sin\gamma_1} = \frac{x - x_L}{\cos\gamma_1} \tag{8}$$

Note that the pixel coordinates of the laser point A_2 in the image plane are u_L and v_L. In the x-y plane, the coordinates of A_2 are (f, $d_x(u_0 - u_L)$). Then, the line F-A_1 is represented by

$$\frac{y}{d_x(u_0 - u_L)} = \frac{x}{f} \tag{9}$$

Combining (8) and (9), the coordinates of point A_1 are derived by

$$x_{A1} = \frac{f(y_L - x_L tg\gamma_1)}{d_x(u_0 - u_L) - ftg\gamma_1} \tag{10}$$

$$y_{A1} = \frac{d_x(u_0 - u_L)(y_L - x_L tg\gamma_1)}{d_x(u_0 - u_L) - ftg\gamma_1} \tag{11}$$

In a similar manner, the coordinates of point B_1, denoted by x_{B1} and y_{B1}, can be derived. Finally, the pan angle of the robot relative to the window frame is given by

$$\theta = arctg(\frac{x_{B1} - x_{A1}}{y_{B1} - y_{A1}}) \tag{12}$$

As seen in Fig. 9, θ denotes the orientation of the robot on the glass, based on which the robot can rotate its waist to reach a desired posture.

Fig. 10. Motion test at the City University of Hong Kong

5. Experiments

The robot was tested in cleaning a glass wall of the academic building at the City University of Hong Kong, as shown in Fig. 10. The robot operation includes: 1) adjusting the orientation by rotating the waist, 2) cleaning the glass wall with brash, and 3) crossing the

window frame from one glass section to another section. The successful demonstrations show that the climbing robot can clean the glass wall automatically and effectively.

When the robot cleans the glass wall, detection of the orientation is important for the robot to move along the desired trajectory, and measurement of the distance between the robot and the window frame is also important to infer the robot to cross the window frame. A series of experiments were performed to evaluate the effectiveness of the visual sensing system in measuring the robot's orientation and the distance between the robot and the window frame.

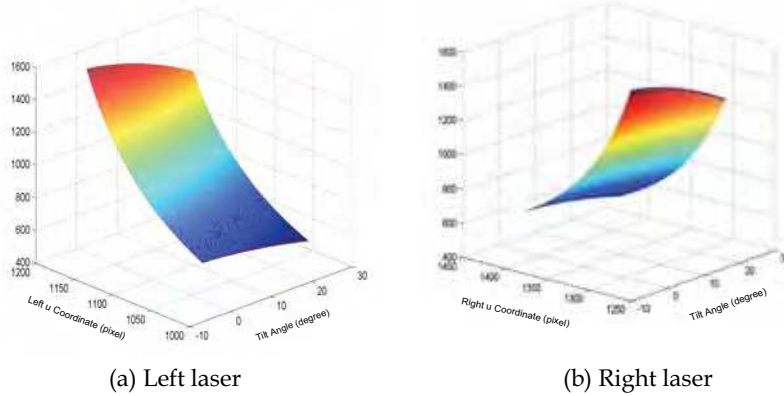(a) Left laser   (b) Right laser

Fig. 11. Distance between the robot and the window frame -- u coordinate of the left/right laser point and tilt angle of the camera

5.1 Measurement of the Robot Position

Firstly, the visual sensing system was calibrated by acquiring images and analyzing u or v coordinates of the laser points when the robot was at different calibration positions on the glass surface. With the least square fitting, the distance between the robot and the window frame could be developed from the calibration as a function of u coordinate of the left laser point u_L (pixel) and the tilt angle of the camera α (degree). The detailed procedures of calibration are listed in the following:

1. Move the robot to an arbitrary position and measure the distance between the robot to the window frame (i.e., the distance d is 100 mm), and then use the camera to acquire the title angle α and the pixel coordinates u_R (and u_L).
2. Move the robot to the other positions and obtain a series of calibration data;
3. Obtain coefficients a_1, a_2, a_3 and β, with the least square fitting method, from equation (7).

Through the above calibration procedures, we obtained $a_1 = 16.67$, $a_2 = -185839.97$, and $a_3 = -1286.21$. Then, the distance is derived from Simoncelli et al. (2000) as

$$d = \frac{16.67\,u_L - 185839.97}{u_L - 1286.21}\cos(\alpha + 9.2^\circ) \ \ (\text{mm}) \tag{13}$$

In a similar manner, the distance d could be developed as the function of u coordinate of the right laser point, i.e.

$$d = \frac{33.09\,u_R + 96310.74}{u_R - 1197.37}\cos(\alpha + 8.9^\circ) \quad (\text{mm}) \tag{14}$$

The distance functions in v coordinate of the two laser points were also developed. After comparison, we found that the distance measurement with u coordinate was more accurate than with v coordinate in this experiment. Figs. 11 (a) and(b) illustrate the relationships described in equations (13) and (14), respectively.

In the following experiments, equation (13) was used to measure the position of the robot on the glass surface. Experimental results of the relationship between the measurement error and the distance measured is shown in Fig. 12, where the squared points denote the measurement errors with different distances, and the solid line denotes a trend of the measurement errors as the distance increases. When the camera pans 90 degrees anti-clockwise, the distance between the robot and the left window frame can be measured. When the camera pans 90 degrees clockwise, the distance between the robot and the right window frame can be measured. To solve the error accumulative problem of the measured distance, the visual sensor needs to be reset after several measurements. Note that the camera distortion may affect the measurement of d. It is seen from Fig. 12 that the measurement error is small (i.e., < 10 mm) when the distance is not large (i.e., <1000 mm). In case of large distance, the camera distortion correction should be considered.
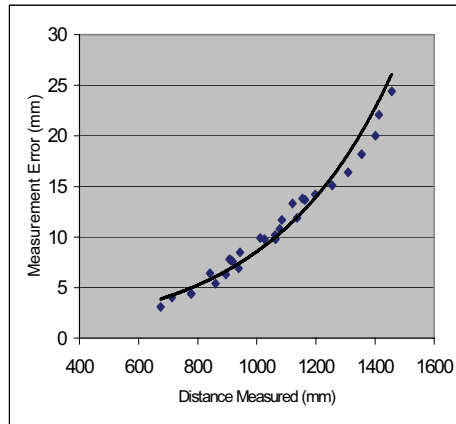

Fig. 12. Trend of the distance measurement errors

5.2 Measurement of the Robot Orientation

The visual sensing system was further calibrated to find the relationship between the robot's orientation and the u coordinates of the left and the right laser points in the image. With the least square fitting, the following relationship can be derived from the calibration:

$$\theta = arctg(\frac{-691.2 \; u_L - 798.34 \, u_R + 1841988.56}{u_L u_R - 1234.92 \, u_L - 1282.83 \, u_R + 1584334.83})$$
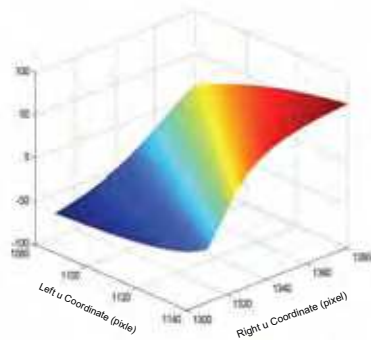(15)

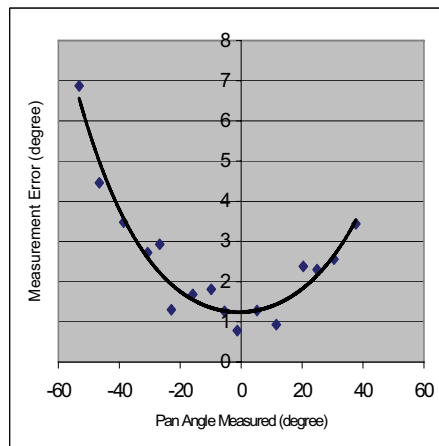Fig. 13. Measurement of the robot orientation based on u coordinates of the left and right laser points

Fig. 14. Trend of orientation-measure errors

Fig. 13 illustrates the relationship between the pan angle θ and the coordinates u_L and u_R.

The relationship between the pan angle and the measurement errors is shown in Fig. 14, where the squared points denote the measurement errors with different orientations, and the solid line denotes a trend of the orientation measurement errors as the pan angle changes. Note that the pan angle error may contribute to the overall measurement error. However, in certain applications, the effect of the pan angle error to the distance measurement is not serious. In our experiment, we found when the robot climbed over 2 m horizontally on the glass surface, the pan angle of the robot is less than 6 degrees.

The orientation of the robot may be affected by the gravitational force, especially when the robot climbs horizontally. When the robot climbed over 2 m horizontally on the glass

surface, the pan angle of the robot was found to be less than 6 degrees in the experiment. When the pan angle was measured to be positive, the robot rotated its waist clockwise to reach the desired horizontal or vertical orientation. When the pan angle was measured to be negative, the robot rotated anti-clockwise until reaching its desired posture.

5.3 Measurement of the Location of the Dirty Spot

The pattern recognition technique was used to find out the dirty spot to be cleaned and then to obtain the image of the laser mark. Equation (14) was used to measure the distance between the robot and the dirty spot. Based on the measured distance and the pan angle of the camera, the location of the dirty spot can be known. The experimental results of locating dirty spots are shown in Table 1.

	ψ (degree)	Tilt Angle (degree)	Right Coordinate u (pixel)	D (mm)	Measure error (x, y) (mm)
1	37	11	1364	798.2	(2.6, 3.7)
2	65	17	1400	633.3	(3.2, 1.6)
3	52	22	1410	577.0	(2.5, 2.1)
4	53	11.6	1370	768.6	(3.5, 2.6)
5	54	5	1325	1066.1	(7.1, 3.4)
6	75	2.4	1311	1205.6	(10.3, 2.0)
7	67	9	1348	890.3	(6.1, 2.0)
8	65	5	1327	1050.1	(7.7, 2.6)
9	78	10.4	1358	830.0	(5.9, 1.4)

Table 1. Experimental results of locating the position of the dirty spot

6. Conclusions

This chapter persents an application of a climbing robot for the glass cleaning service. The robot is constructed by two rodless cylinders and a rotation cylinder. The robot can adjust its orientation to maintain in the desired trajectory path. After finishing the cleaning work in one section of the glass wall, the robot can cross the window frame to enter another section. A visual sensing system, which is composed of an omnidirectional CCD camera and two laser diodes, is applied to measure the robot's position and orientation on the glass wall. Experiments demonstrate that with the assistance of the proposed motion planning and visual sensing technologies, the climbing robot can perform cleaning work on the glass wall effectively. Future work will be toward developing more efficient motion control system and reducing size/weight of the climbing robot.

7. Acknowledgement

8. References

Balaguer, C.; Gimenez, A.; Pastor, J. M. V.; Padron, M. & Abderrahim, M. (2000). Climbing autonomous robot for inspection applications in 3D complex environments. *Robotica*, Vol. 18, No. 3, pp. 287-297.

Boissonnat, J. D.; Devillers, O. & Lazard, S. (2000). Motion planning of legged robots. *SIAM Journal on Computing*, Vol. 30, No. 1, pp. 218-246.

Chen, C. H.; Kumar V. and Luo, Y. C. (1999). Motion planning of walking robots in environments with uncertainty. *Journal of Robotic Systems*, Vo. 16, No. 10, pp. 527-545.

Egerstedt M. and Hu, X. (2002). A hybrid control approach to action coordination for mobile robots. *Automatica*, Vol. 38, No 1, pp. 125-130.

Hasegawa, Y.; Arakawa T. & Fukuda, T. (2000). Trajectory generation for biped locomotion robot. *Mechatronics*, Vol. 10, No. 1-2, pp. 67-89.

Hert S. & Lumelsky, V. (1999). Motion planning in R^3 for multiple tethered robots. *IEEE transactions on robotics and automation*, Vol. 15, No. 4, pp. 623-639.

Kurazume, R. and Hirose, S. (2000). Development of a cleaning robot system with cooperative positioning system. *Autonomous Robots*, Vol. 9, No. 3, pp. 237-246.

Lamiraux, F. & Laumond, J. P. (2001). Smooth motion planning for car-like vehicles. *IEEE Transactions on Robotics and Automation,* Vol. 17, No. 4, pp. 498-501.

La Rosa, G.; Messina, M.; Muscato, G. & Sinatra, R. (2002). A low-cost lightweight climbing robot for the inspection of vertical surfaces. *Mechatronics*, Vol. 12, No. 1, pp. 71-96.

Ma, Y.; Kosecka, J. and Sastry, S. S. (1999). Vision guided navigation for a nonholonomic mobile robot. *IEEE Trans. Robot. Automat.*, Vol. 15, No. 3, pp. 521-536.

Maeda, S.; Kuno, Y. & Shirai, Y. (1997). Mobile robot localization based on eigenspace analysis. *Systems and Computers in Japan*, Vol. 28, No. 12, pp. 11-21.

Malis, E.; Chaumette, F. and Boudet, S. (2000). Multi-cameras visual servoing. *Proc. IEEE Conf. Robot. Automat*, pp. 3183-3188, San Francisco, CA, USA, April 2000.

Malis, E.; Chaumette, F. & Boudet, S. (1999). 2-1/2-D visual servoing. *IEEE Trans. Robot. Automat.*, Vol. 15, No. 2, pp. 238-250.

Mosemann H. and Wahl, F. M. (2001). Automatic decomposition of planned assembly sequences into skill primitives. *IEEE Transactions on Robotics and Automation*, Vol. 17, No. 5, pp. 709-718.

Simoncelli, M.; Zunino, G.; Christensen, HI and Lange, K. (2000). Autonomous pool cleaning: Self localization and autonomous navigation for cleaning. *Autonomous Robots*, Vol. 9, No. 3, pp. 261-270.

Sun, D., Zhu, J., Lam, C. and Tso, S. K. (2004). A visual sensing application to a climbing cleaning robot on the glass surface. *Mechatronics* , Vol. 14, pp. 1089-1104.

Zhu, J.; Sun D. and Tso, S. K. (2002). Development of a tracked climbing robot. *Journal of Intelligent and Robotic Systems*, Vol. 35, No. 4, pp. 427-444.

Zhu, J.; Sun D. and Tso, S. K. (2003). Application of a service climbing robot with motion planning and visual sensing . *Journal of Robotic Systems*, Vol. 20, No. 4., pp. 189-199.

Climbing and Walking Robots: towards New Applications

Edited by Houxiang Zhang

ISBN 978-3-902613-16-5

Hard cover, 546 pages

Publisher I-Tech Education and Publishing

Published online 01, October, 2007

Published in print edition October, 2007

With the advancement of technology, new exciting approaches enable us to render mobile robotic systems more versatile, robust and cost-efficient. Some researchers combine climbing and walking techniques with a modular approach, a reconfigurable approach, or a swarm approach to realize novel prototypes as flexible mobile robotic platforms featuring all necessary locomotion capabilities. The purpose of this book is to provide an overview of the latest wide-range achievements in climbing and walking robotic technology to researchers, scientists, and engineers throughout the world. Different aspects including control simulation, locomotion realization, methodology, and system integration are presented from the scientific and from the technical point of view. This book consists of two main parts, one dealing with walking robots, the second with climbing robots. The content is also grouped by theoretical research and applicative realization. Every chapter offers a considerable amount of interesting and useful information.

How to reference

In order to correctly reference this scholarly work, feel free to copy and paste the following:

Dong Sun, Jian Zhu and Shiu Kit Tso (2007). A Climbing Robot for Cleaning Glass Surface with Motion Planning and Visual Sensing, Climbing and Walking Robots: towards New Applications, Houxiang Zhang (Ed.), ISBN: 978-3-902613-16-5, InTech, Available from:
http://www.intechopen.com/books/climbing_and_walking_robots_towards_new_applications/a_climbing_robot_for_cleaning_glass_surface_with_motion_planning_and_visual_sensing

INTECH
open science | open minds